

## HEX TORI FROM SQUARE TORI

MIRCEA V. DIUDEA<sup>a\*</sup>, BAZIL PARV<sup>b</sup> and OLEG URSU<sup>c</sup>

<sup>a</sup> Faculty of Chemistry and Chemical Engineering

<sup>b</sup> Department of Computer Science, Faculty of Mathematics  
Babes-Bolyai University, 3400 Cluj, Romania

<sup>c</sup> Department of Chemistry, Cleveland State University  
2121 Euclid Avenue, Cleveland OHIO 44115 USA

**ABSTRACT.** Hex and other tiled tori can be derived from square tori. This way of building toroidal fullerenes is a versatile one, enabling various tilings: rhomboidal C<sub>4</sub>, polyhex C<sub>6</sub>, C<sub>4</sub>C<sub>8</sub>, azulenic C<sub>5</sub>C<sub>7</sub> as well as twisted lattices. The stability of polyhex toroids is discussed in terms of molecular mechanics energy.

### INTRODUCTION

Among the carbon allotropes, the only orientable closed surface entirely coverable by a bezenoid lattice is the torus. The polyhedral (combinatorial) torus obeys the Euler theorem:<sup>1</sup>

$$N - E + F = 2 - 2g \quad (1)$$

( $N$ ,  $E$ ,  $F$ ,  $g$  being respectively the number of vertices, edges, faces, and genus – for the torus  $g = 1$ ). Formula is useful for checking the consistency of an assumed structure.

"Circle crops" structures were first observed by Liu *et al.*<sup>2</sup> and then by other groups.<sup>3-5</sup> Martel *et al.*<sup>5</sup> argued that the observed rings were coils rather than perfect tori, but these structures have continued to attract a multitude of theoretical studies, dealing with construction, mathematical and physical properties of graphitic tori.<sup>6-14</sup>

This paper describes a novel way of generating polyhex tori, starting from quadrilateral tori. Several cutting procedures and transformations of the square toroidal nets are proposed in the view of obtaining chemically significant lattices. The stability of polyhex tori, the main toroidal objects herein generated, is discussed in terms of the MM+ energy.

### SQUARE TORI GENERATION

Covering a torus by hexagons is achieved mainly by the well-known graphite zone-folding.<sup>11-16</sup> The method finds an equivalent planar parallelogram, tiled by a polyhex lattice. The graphite sheet is folded to form a tube and finally

the two ends of the tube are glued in order to form a torus. A torus  $T_{p,q,t}$  thus obtained is completely defined by four integers, reducible to three parameters:<sup>14,16</sup>  $p$  and  $q$  count the hexagons stacked in a  $p \times q$ -parallelogram and  $t$  is the twisting parameter, *i.e.*, the number of hexagons offset before final pasting.

An alternative to the parallelogram procedure is the AME (*i.e.*, adjacency matrix eigenvectors).<sup>17-20</sup> Our construction starts from a square net embedded on the toroidal surface.<sup>21-24</sup> A  $c$ -fold cycle, circumscribed to a tube section of radius  $r$ , is circulating along the toroidal circle, of radius  $R > r$  (Figure 1). Its subsequent  $n$  images, equally spaced and joined with edges, point by point, form a polyhedral torus tiled by a square pattern. The position of each of the  $n$  images of the circulant around the large circle is characterized by angle  $\theta$  while angle  $\varphi$  locates the  $c$  points of the circulant around the small circle. In all,  $c \times n$  points are generated.

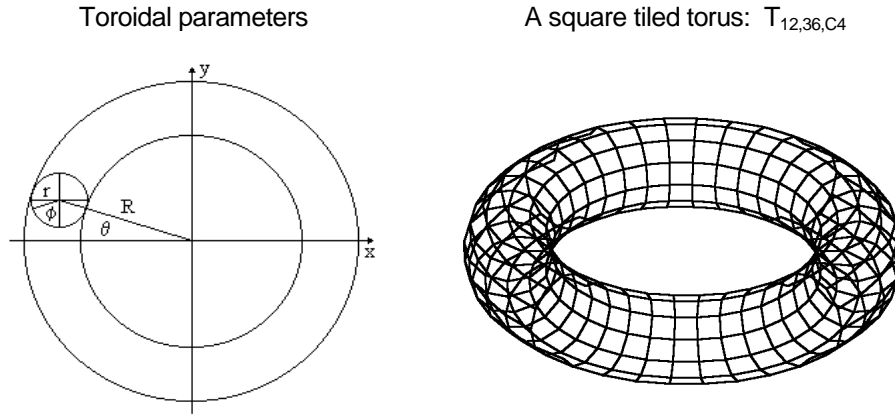


**Figure 1.** Construction of a toroidal surface.

The parameters are calculated by the following formulas:

$$P(x, y, z) : \quad (2)$$

$$x = \cos(\theta)(R + r \cos \varphi)$$

$$y = \sin(\theta)(R + r \cos \varphi)$$

$$z = r \sin \varphi$$

$$\theta_i = \frac{2\pi}{n} i \quad ; \quad i = 0, \dots, n-1$$

$$\varphi_j = \frac{2\pi}{c} j \quad ; \quad j = 0, \dots, c-1$$

## HEX TORI FROM SQUARE TORI

The problem is *how to transform a square net* covering the toroidal surface into patterns of chemical interest. At this stage, the genuine length of  $r$  and  $R$  is not a matter.

The square lattice generated as described above is a torus,  $C_4[c,n]$  completely defined by two integers:  $c$ —dimension of the tube and  $n$ —dimension of the torus (*i.e.*, the combinatorial dimensions of the square toroidal net). The subscript in  $C_4$  specifies the size of the polygonal tiling pattern.

In case of single-wall tori, the square net consists of  $c \times n$  vertices,  $c \times n$  squares and  $4 \times c \times n / 2$  edges, 4 being the vertex degree of the net (which is a regular graph). The above relations come out as a consequence of Euler's formula.

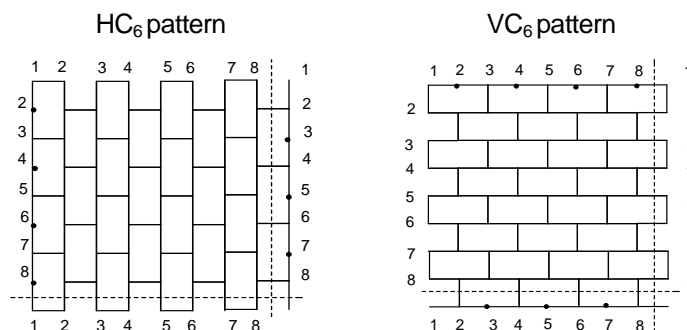
### HEX TORI FROM SQUARE TORI

A cutting operation consists of deleting appropriate edges in a square lattice in order to produce some larger polygonal faces. By deleting each second *horizontal* edge and alternating edges and cuts in each second row it results in a standard  $HC_6$  pattern (Figure 2 (a), top).

After optimizing by a molecular mechanics program, a phenacenic pattern appears on the torus (Figure 2 (a), bottom).

A *vertical action* of the above algorithm leads to a standard  $VC_6$  pattern (Figure 2, (b)). It means that, after optimization, an acenic pattern is obtained (Figure 2 (b), bottom).

Note that each hexagon consumes exactly two squares in the square-like lattice. By construction, the number of hexagons in the  $HC_6$  pattern is half the number of squares on dimension  $c$  of the torus  $HC_6[c,n]$  while in the  $VC_6[c,n]$  torus the reduced number of hexagons appears on dimension  $n$ . Recall that, the above cutting procedure leaves unchanged the number of vertices in the original square torus. The name of a polyhex torus, thus generated, has to remind the *type of cutting* (H or V), as well as the *size of cycles* occurring in a given pattern. Figures 3 illustrates two isomeic objects originated in  $C_4[12,24]$ . Within this paper no twisted, chiral polyhex tori are discussed.



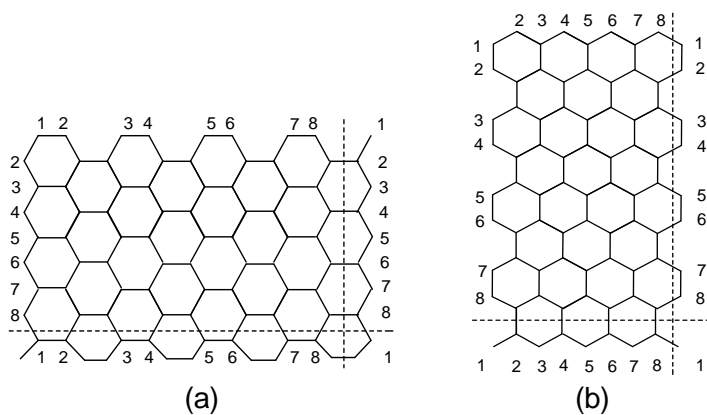
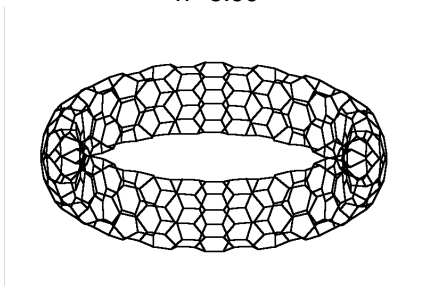


**Figure 2.** Standard  $C_6$  patterns and their optimized forms.

$HC_6[12,36]$  (side)  
 $h=5.90$



$HC_6[12,36]$  (top)  $N = 432$   
 $d=2.90$ ;  $D = 23.91$

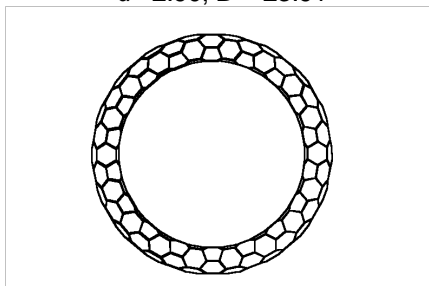
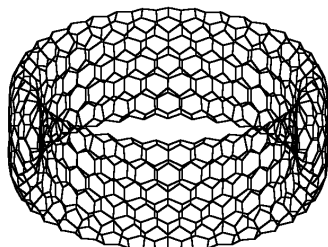


**Figure 3a.** Polyhex tori  $HC_6[c,n]$ : height  $h$ , tube diameter  $d$  and torus diameter  $D$ , respectively (in Angstroms)

$VC_6[12,72]$  (side)  
 $h=11.44$



$VC_6[12,72]$  (top)  $N = 864$   
 $d = 3.51$ ;  $D = 27.52$

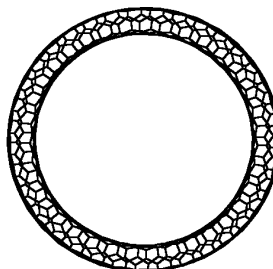


**Figure 3b.** Polyhex tori  $VC_6[c,n]$ : height  $h$ , tube diameter  $d$  and torus diameter  $D$ , respectively (in Angstroms)

# MOLECULAR MECHANICS CALCULATIONS

Our TORUS software package enabled us to generate huge tori, up to 20,000 atoms, which could be optimised by a molecular mechanics procedure.

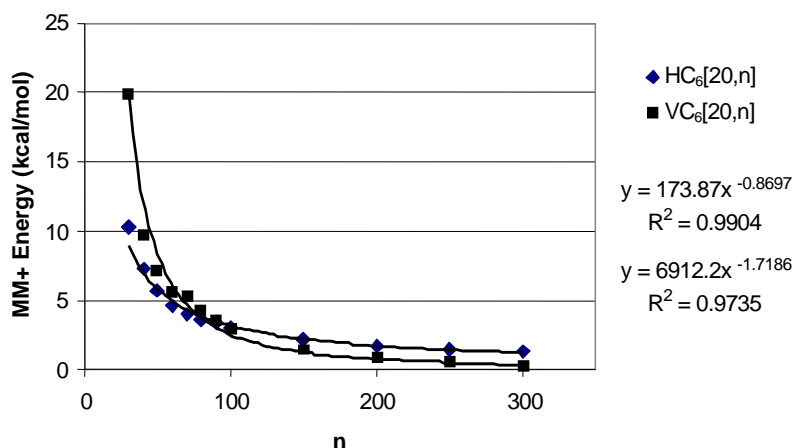


**Figure 4.** Plot of MM+ energy per atom vs the  $n$ -dimension

The MM+ energy per atom decreases as  $n$  (*i.e.*, the central hollow) increases, by a power function (Figure 4). The tori of V-series are more stable than those of H-series.

Note that the MM+ energy for C<sub>60</sub> is about 4.454 kcal/mol, value reached in HC<sub>6</sub>[20,n] series at more than 120 atoms while in VC<sub>6</sub>[20,n] series around 160 atoms. However, in toroids with thousand atoms, the MM+ energy lowers very much, as shown in Table 1.

**Table 1.**

MM+ energy per atom (kcal/mol) in tori of series [20,n]

| $n$ | MM+ for H-series |        | MM+ for V-series |         |
|-----|------------------|--------|------------------|---------|
|     | Tori             | Tubes  | Tori             | Tubes   |
| 20  | 17.7158          | 1.0427 | 36.3829          | -0.7782 |
| 30  | 10.3547          | 1.0313 | 19.9559          | -0.8227 |
| 40  | 7.2618           | 1.0256 | 9.7139           | -0.8450 |
| 50  | 5.6703           | 1.0222 | 7.1764           | -0.8584 |
| 60  | 4.6234           | 1.0212 | 5.5514           | -0.8673 |
| 70  | 4.0344           | 1.0183 | 5.3005           | -0.8737 |
| 80  | 3.6848           | 1.0148 | 4.2428           | -0.8785 |
| 90  | 3.3578           | 1.0181 | 3.4806           | -0.8822 |
| 100 | 3.0931           | 1.0172 | 2.9123           | -0.8850 |
| 150 | 2.1789           | 1.0135 | 1.4550           | -0.8941 |
| 200 | 1.7113           | 1.0149 | 0.8847           | -0.8986 |
| 250 | 1.4706           | 1.0120 | 0.6008           | -0.9010 |
| 300 | 1.3348           | 1.0111 | 0.2310           | -0.9029 |

The energy of the corresponding open tubes is even less, for V-tubes (Table 1) approaching to the graphite sheet value (about (-) 1.85 kcal/mol).

Strain energy (per atom) is here defined as the difference between the energy of a torus minus the energy of the corresponding open tube. Strain energy was found proportional to the diameters ratio:

$$S = \frac{d}{D} \quad (3)$$

where  $d$  and  $D$  are given in number of hexes. Thus, the two series: H and V show different strain energy laws:

$$d_{HC_6[20,n]} = \frac{c}{2\pi}; \quad D_{HC_6[20,n]} = \frac{n}{\pi}; \quad S_{HC_6[20,n]} = \frac{c}{2n} \quad (4)$$

$$d_{VC_6[20,n]} = \frac{c}{\pi}; \quad D_{VC_6[20,n]} = \frac{n}{2\pi}; \quad S_{VC_6[20,n]} = \frac{2c}{n} \quad (5)$$

Despite this difference, the same trend appeared: the strain energy decreases by enlarging the torus central hollow (*i.e.*, by decreasing the  $d/D$  ratio). The excellent correlating equations given in Figure 5 support the strain energy as a function of  $d/D$  ratio.

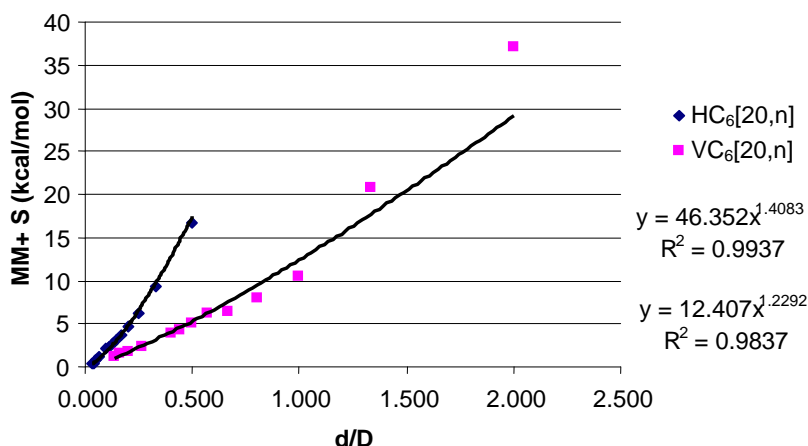


**Figure 5.** Plot of strain energy  $S$  vs the  $d/D$  ratio

The  $d/D$  dependency of the strain energy is in disaccord with that reported by Han<sup>25</sup> which found it to be a of  $1/D^2$  (for a given tube dimension). The author reported the following features of polyhex toroids, as  $D$  increases:

- (i) a buckling tube (for  $10\text{nm} < D < 20\text{ nm}$ ), with oscillating energy minima and migrating buckle position;
- (ii) an elliptic cross section tube (for medium  $D$  valued, *e.g.*,  $D > 20\text{ nm}$ , in case of torus (8,8)), as a transition state, and
- (iii) a perfect circular tube and an energetically stable torus (for higher  $D$  values).

## HEX TORI FROM SQUARE TORI

In our approach, the same stages were observed. H-series approaches the circular cross-section shape at  $HC_6[20,500]$  while in the V-series at  $VC_6[20,1000]$ , a normal result keeping in mind that the V-torus is twice thicker than the corresponding H-torus. Note that our tori are next huge objects ( $20 \times 1000 = 20,000$  atoms) after the largest 30,000 atoms reported by Han, in his NAS report.<sup>25</sup>

Figure 6 illustrates some different shapes of polyhex tori. Observe the "elongated" cross-section<sup>26</sup> in case of V-tori.

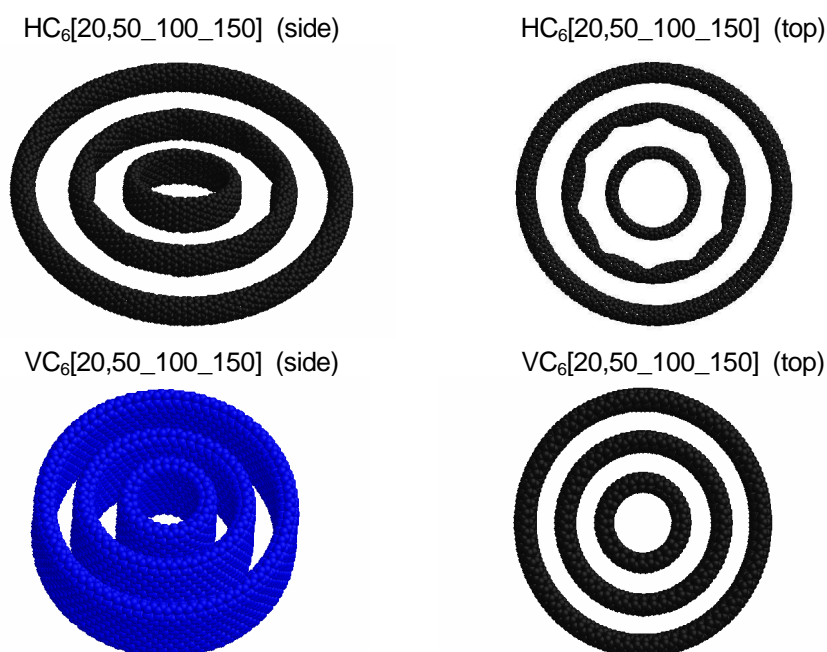


**Figure 6.** A collection of polyhex tori.

MM+ calculations have been performed on the HiperChem software package.<sup>27</sup>

### CONCLUSIONS

Generation of hex tori from square tori is a third major route, along with the graphite zone - folding and adjacency matrix eigenvectors methods. Our method is far more versatile, enabling various polygonal coverings.<sup>28-30</sup>

A  $d/D$  dependency of the strain energy obtained by us is in disaccord with the previously reported  $1/D^2$  dependency. Very large polyhex toroids approach to the MM+ energy of graphite.

**ACKNOWLEDGEMENT.** This paper was supported by the Romanian CNCSIS GRANT 2003.

## REFERENCES

1. L. Euler, *Comment. Acad. Sci. I. Petropolitanae*, **1736**, 8, 128-140.
2. J. Liu, H. Dai, J. H. Hafner, D. T. Colbert, R. E. Smalley, S. J. Tans, and C. Dekker, *Nature*, **1997**, 385, 780-781.
3. M. Ahlskog, E. Seynaeve, R. J. M. Vullers, C. Van Haesendonck, A. Fonseca, K. Hernadi, and J.B. Nagy, *Chem. Phys. Lett.*, **1999**, 300, 202-206.
4. R. Martel, H. R. Shea, and Ph. Avouris, *Nature*, **1999**, 398, 299-299.
5. R. Martel, H. R. Shea, and Ph. Avouris, *J. Phys. Chem., B*, **1999**, 103, 7551-7556.
6. D. Babić, D. J. Klein, and T. G. Schmalz, *J. Mol. Graphics Modell.*, **2001**, 19, 222-231.
7. A. Ceulemans, L. F. Chibotaru, and P. W. Fowler, *Phys. Rev. Lett.*, **1998**, 80, 1861-1864.
8. J. K. Johnson, B. N. Davidson, M. R. Pederson, and J. Q. Broughton, *Phys. Rev., B*, **1994**, 50, 17575-17582.
9. V. Meunier, Ph. Lambin, and A. A. Lucas, *Phys. Rev., B*, **1998**, 57, 14886-14890.
10. M. F. Lin and D. S. Chuu, *Phys. Rev., B*, **1998**, 57, 6731-6737.
11. E. C. Kirby, *Croat. Chem. Acta*, **1993**, 66, 13-26
12. E. C. Kirby, R. B. Mallion, and P. Pollak, *J. Chem. Soc. Faraday Trans.*, **1993**, 89, 1945-1953.
13. A. Ceulemans, L. F. Chibotaru, S. A. Bovin, and P. W. Fowler, *J. Chem. Phys.*, **2000**, 112, 4271-4278.
14. D. Marušić and T. Pisanski, *Croat. Chem. Acta*, **2000**, 73, 969-981.
15. D.J. Klein, *J. Chem. Inf. Comput. Sci.*, **1994**, 34, 453-459.
16. E. C. Kirby and P. Pollak, *J. Chem. Inf. Comput. Sci.*, **1998**, 38, 66-70.
17. T. Pisanski and J. Shawe-Taylor, *J. Chem. Inf. Comput. Sci.*, **2000**, 40, 567-571.
18. A. Graovac, D. Plavšić, M. Kaufman, T. Pisanski, and E. C. Kirby, *J. Chem. Phys.*, **2000**, 113, 1925-1931.
19. A. Graovac, M. Kaufman, T. Pisanski, E. C. Kirby, and D. Plavšić, *J. Chem. Phys.*, **2000**, 113, 1-7.
20. I. Laszlo, A. Rassat, P. W. Fowler, and A. Graovac, *Chem. Phys. Lett.*, **2001**, 342, 369-374.
21. M. V. Diudea and A. Graovac, *Commun. Math. Comput. Chem. (MATCH)*, **2001**, 44, 93-102.
22. M. V. Diudea, I. Silaghi-Dumitrescu, and B. Parv, *Commun. Math. Comput. Chem. (MATCH)*, **2001**, 44, 117-133.
23. M. V. Diudea and E. C. Kirby, *Fullerene Sci. Technol.*, **2001**, 9, 445-465.
24. M. V. Diudea, *Bull. Chem. Soc. Japan*, **2002**, 75, 487-492.
25. J. Han, *Chem. Phys. Lett.*, **1998**, 282, 187-191.
26. S. Itoh and S. Ihara, *Phys. Rev., B*, **1993**, 48, 8323-8328.
27. HyperChem [TM], release 4.5 for SGI, © 1991-1995, HyperCube, Inc.
28. M. V. Diudea, *Fullerenes, Nanotubes, Carbon Nanostruct.*, **2002**, 10, 273-292.
29. M. V. Diudea, *Phys. Chem., Chem. Phys.*, **2002**, 4, 4740-4746.
30. M. V. Diudea, B. Parv and E. C. Kirby, *Commun. Math. Comput. Chem. (MATCH)*, **2003**, 47, 53-70.